Original Manuscript

JOURNAL OF COMPOSITE MATERIALS

Journal of Composite Materials
2024, Vol. 0(0) 1–11

DOI: 10.1177/00219983241238057
journals.sagepub.com/home/jcm
Sage

Effects of silver nanowires and their surface modification on electromagnetic interference, transport and mechanical properties of an aerospace grade epoxy

Merve Özkutlu Demirel[1], Mahide B Öztürkmen[1], Müzeyyen Savaş[2], Evren Mutlugün[2], Talha Erdem[2] and Yahya Öz[1]

Abstract

The aerospace industry has progressively grown its use of composites. Electrically conductive nanocomposites are among important modern materials for this sector. We report on a bulk composite containing silver nanowires (AgNW) and an aerospace grade epoxy for use in carbon fiber reinforced polymers (CFRPs). AgNWs' surfaces were also modified to enhance their ability to be dispersed in epoxy. Composites were obtained by use of three-roll milling which is of major interest for industrial applications, especially for the aerospace sector, since the process is scalable and works for aerospace grade resins with high curing temperatures. Our main objective is to improve the electromagnetic interference (EMI) shielding performance of CFRPs via improving the properties of the resin material. The addition of AgNWs did not considerably alter the flexural strength of the epoxy, however the composite with surface-modified AgNWs has a 46 % higher flexural strength. Adding AgNWs over a low threshold concentration of 0.05 wt% significantly enhanced the electrical conductivity. Conductivities above the percolation threshold lie around 10^2 S/m. At a concentration of 5 wt% AgNW, the EMI shielding efficiency (SE) of epoxy increased from 3.49 to 12.31 dB. Moreover, the thermal stability of the epoxy was unaffected by AgNWs. As a result, it was discovered that (surface modified) AgNWs improved the (multi-functional) capabilities of the aerospace grade epoxy resin which might be used in CFRPs to further enhance properties of composites parts, demonstrating suitability of AgNWs' as a reinforcement material in aerospace applications.

Keywords

Aerospace applications, electromagnetic interference shielding, epoxy, multifunctional nanocomposites, silver nanowires

Introduction

Utilization of polymer matrix composites in the aerospace industry has increased rapidly over the past few decades.[1–4] An important class of contemporary materials includes electrically conductive polymer nanocomposites with desired mechanical and/or thermal and/or electrical characteristics, such as EMI shielding, thermal stability, flexibility and adhesive strength.[5–7]

Electromagnetic interference shielding materials, which suppress the transmission of electromagnetic waves through reflection and absorption, are critical for many systems involving electronic equipment.[8,9] For both military and commercial applications such as Doppler radar, weather radar, television picture transmission, and telephone microwave relay systems, *X*-band EMI shielding in the range of 8.2 – 12.4 *G*Hz is of critical importance. Metals were being used as matrix material in aircrafts for several decades until low-density, carbon fiber reinforced thermosets provided higher mechanical performance.[10–12] However, metals still typically make up conventional *X*-band EMI shielding materials because of their superior electrical conductivity since, compared to an aluminum part, CFRPs have a poor electrical conductivity of roughly 10^{-2} S/m.

[1]Advanced Composite Materials Technology Center, R&D and Technology Directorate, Turkish Aerospace, Ankara, Turkey
[2]Department of Electrical & Electronics Engineering, Faculty of Engineering, Abdullah Gül University, Kayseri, Turkey

Corresponding author:
Merve Özkutlu Demirel, Turkish Aerospace, Ankara 06980, Turkey.
Email: merve.ozkutludemirel@tai.com.tr

Data Availability Statement included at the end of the article

Hence, the real challenge is to increase CFRP's conductivity to satisfy EMI requirements and to protect the aircraft against lighting strikes.[13,14]

Owing to their appealing qualities like light weight, superior flexibility, high chemical stability, and simplicity of processing and shape, conductive polymer composites (CPCs) step forward as effective EMI shielding materials.[8,15] Microwave radiation may or may not be absorbed by virgin polymers depending on whether they are conducting or insulating by nature. Polymer composites created by adding conductive fillers have drawn a lot of attention recently as EMI shielding materials.[16,17] However, it is still difficult to achieve high electrical conductivity with mechanical properties and good thermal stability since it necessitates using high amounts of conductive nanofillers within the polymer matrix, which frequently degrades physical properties of composites.[5,18,19]

The structure of composites has an obvious influence on the corresponding electrical conductivity and is thus inferred to have a significant effect on the EMI shielding performance. Because they have a lower percolation threshold and better shielding capabilities, high aspect ratio nanofillers like carbon nanotubes (CNTs) are preferred for creating composites.[17,20,21] One-dimensional AgNWs are another class of excellent conducting fillers for producing polymer composites for *X*-band EMI shielding.[22,23] Conductive AgNW/polyaniline (PANI) nanocomposites for instance have shown an excellent performance of above 50 *d*B over a wide bandwidth of 1.2 *G*Hz.[17] Silver nanoparticles (AgNPs) and epoxy composite films loaded with AgNWs were compared in EMI shielding efficiency over the frequency range of 3 – 17 *G*Hz. Remarkably, it was observed that when AgNWs were added instead of AgNPs, the silver content could be lowered by four times.[24] Core-shell-type polyaniline-silver nanosheets were studied in 2021.[25] An EMI SE of about 70 *d*B between 4 and 12 *G*Hz was observed due to conductivities in the range of $10^5 - 10^6$ S/m which are typically observed for metals. Note that silver was also used in the literature in different other forms like coatings and meshs to achieve EMI shielding properties.[26]

The EMI shielding capabilities of bulk composites with silver nanowires, however, are not well covered in the literature. In order to address the explained challenges, in this study we aim to obtain a composite using an aerospace grade epoxy resin and AgNWs which has the potential to be further processed by reinforcing with carbon fibers. It would be advantageous to enhance properties of these CFRPs by incorporating a resin with higher electrical conductivity, which also exhibits electromagnetic interference shielding properties. Therefore, the main purpose of this study is to increase the electrical conductivity of the resin, thus improve its EMI shielding performance while maintaining mechanical as well as thermal properties resulting in multifunctional characteristics. For this purpose, AgNWs were dispersed in an epoxy resin at 0.05, 0.1, 0.25 and 0.5 wt% amounts. Microstructure, EMI shielding mechanisms, thermal properties and mechanical strengths of the obtained composites were systematically investigated. In order not to sacrifice mechanical properties, the AgNW concentration was kept at the maxiumum value of 0.5 wt%. At higher concentrations nanoparticles may show agglomeration which forms stress concentrated regions that might cause earlier deformation of the matrix under loads.[6,27] However, an epoxy AgNW composite with 5 wt% AgNWs was produced to investigate effects of the AgNW amount on electromagnetic shielding properties of the composite. Moreover, a specific reinforcement ratio was chosen for preparing surface modified AgNW (m-AgNW) epoxy composites to improve the homogeneity of the composites while studying its effects on varying properties of the structure. By considering the reinforcement ratio of the samples produced within the scope of this study, it was evaluated that the optimum ratio for AgNW was 0.25 wt%. Therefore, the composite with modified AgNWs was also studied for this concentration.

Materials and method

Materials

For synthesis of AgNWs; polyvinylpyrrolidone (PVP) powder with a molecular weight of approximately 40,000, silver nitrate ($AgNO_3$), sodium chloride (NaCl), potassium bromide (KBr) and ethylene glycol (EG) with purities of 99.0, 99.5, 99.0 and 99.0 %, respectively, ethanol absolute purchased from ISOLAB with a purity of ≥99.9 %, acetone from Merck and methanol with a purity of ≥99.7 % were used. All chemicals and reagents were purchased from Sigma-Aldrich unless otherwise stated and used without further purification. An aerospace grade epoxy resin; Araldite LY5052 and Aradur HY5052 hardener were supplied from Huntsman for the production of polymer composites. For the surface modification of AgNWs mercaptopropionic acid (MPA) with a purity of ≥99 % and dimethylformamide (DMF) with a purity of ≥99.8 % (Merck) were used.

Synthesis of AgNWs

AgNWs were synthesized through the polyol process which is a solution processing method developed by Kim et al.[28] First, 200 *m*L of EG and 6.68 g of PVP were mixed in a two-necked flat-bottom flask and stirred at 350 r/min with a magnetic stirrer until PVP was completely dissolved in EG. The mixture was heated to 170°C. 0.2 g NaCl, 0.1 g KBr and 2.793 g $AgNO_3$ were added to the solution when it reached 170°C and stirring was continued. Afterwards, the solution was held at 170°C for 4 h to allow the AgNW

growth process to occur. Subsequently, it was cooled to room temperature by placing the flask in a water bath. To get rid of impurities, the nanowire solution was centrifuged with methanol and acetone at a 3:1 ratio twice at 5000 r/min for 10 min. Collected AgNWs were finally dispersed in ethanol.

Surface modification of AgNWs

34.5 *m*L of the AgNW – ethanol solution (20 *m*g/*m*L) were centrifuged to remove ethanol. 2.07 g MPA were added into 1 L DMF. Afterwards, AgNWs were added into the solution and stirred using a magnetic stirrer for 24 h at room temperature. Subsequently, the solution was centrifuged and precipitated AgNWs were dispersed in deionized water.

Production of epoxy – AgNW composites

A three-roll mill device (Torrey Hills Technologies) was employed to disperse AgNWs in the epoxy resin. For this purpose, 0.05, 0.10, 0.25, and 0.50 wt % AgNWs were mixed with the resin and operated with the three-roll-mill for five cycles. The rolling speed was 30 r/min and the gap size between adjacent rolls was 50 μm. Next, the resin was mixed with the hardener and than poured into stainless steel metal molds. A mold release product was used to facilitate the removal of the samples from the mold after mixtures were prepared. The curing process was carried out in an oven at room temperature for 30 min and subsequently crosslinking was achieved at 120°C for 4 h. Finally, cured samples were cooled to room temperature.

Characterization

Using a Bruker/Vertex70 FTIR spectrometer, the nanocomposites' Fou-rier–transform infrared (FTIR) spectra were recorded between 400 and 4000 $c\mathrm{m}^{-1}$. Under nitrogen flow, a specimen was heated from ambient temperature to 900°C at a rate of 10°C/min in order to perform a thermal gravimetric analysis (TGA) using a TA Instrument Q500. A TA Instrument Q2000 device was applied to analyze AgNW nanocomposites using differential scanning calorimetry (DSC). In order to determine the glass transition temperature (T_g) of the neat epoxy and nanocomposites, samples were heated from room temperature to 300°C at a rate of 10°C/min while being in a nitrogen atmosphere. Nano-Magnetic Instruments ezHEMs were used to conduct Hall effect tests at room temperature with a 0.1 *m*A source current present. For the three point bending flexural test, samples of 80 × 10 × 4 $m\mathrm{m}^3$ in the shape of bars were manufactured in accordance with the American Society for Testing and Materials (ASTM) D2344 standard. Using a Shimadzu Autograph AG-IS Universal Testing Machine, the flexural strength of each sample was evaluated. The surface morphology of the nanocomposites was studied and information on the nanowires inside the epoxy matrix was obtained using a FEI Quanta 200 FEG field emission scanning electron microscope (SEM). Images were taken at 500, 1250, 2500, 5000, and 10,000 magnifications at 10 *k*V to complete the SEM investigation of the samples. Energy-dispersive X-ray spectroscopy (EDS) analyses were conducted with a Hitachi SU5000 Field Emission SEM with an Oxford X-MaxN 80 model EDS detector. EMI SE was tested using the ASTM D5568 method using a Network Analyzer from Keysight with the waveguide method. Measured frequencies ranged from 8.2 to 12 *G*Hz. Percent transmission *T*, reflection *R* and absorption *A* values were calculated using the transmission and reflection in *d*B (T_{dB} and R_{dB}) according to equation (1),[29] i.e.,

$$T = 100\left(10^{\frac{T_{dB}}{20}}\right)^2, R = 100\left(10^{\frac{R_{dB}}{20}}\right)^2, A = 100 - T - R \quad (1)$$

EMI shielding effectiveness SE values in *d*B were also calculated using equation (2),[30] i.e.,

$$\mathrm{SE} = 20\log|S_{21}| \quad (2)$$

Results and discussion

Properties of AgNWs

Over the years, researchers have suggested a number of techniques for synthesizing AgNWs.[31] Since the uniformity and crystal quality of the nanowires affect electrical and optical properties of AgNW films, the main goal has been to produce uniform AgNWs with high yield. In this work, we preferred to employ the polyol technique[32] because it offers better dimension control, low production cost, higher yields, and more uniformity.[31] By following this technique, we aimed for achieving reasonable dimensions suitable for electric conductivity and optical transparency while keeping the production costs manageable.

The SEM image presented in Figure 1 shows that synthesized nanowires are straight with an average diameter of 43 *n*m and length larger than 7 μm.In addition to the electron microscopy, we also employed optical characterization since optical features of synthesized AgNWs carry information on their morphology. As shown in Figure 2, the absorption spectrum of AgNWs dispersed in ethanol have a weak peak at 350 *n*m, which was attributed to the longitudinal mode or the out-of-plane quadrupole mode and mainly related to the diameter of nanowires. The stronger peak at 380 *n*m was ascribed to plasmon resonance peaks of silver due to the transverse mode of nanowires, which can be related to the length of nanowires.[33,34]

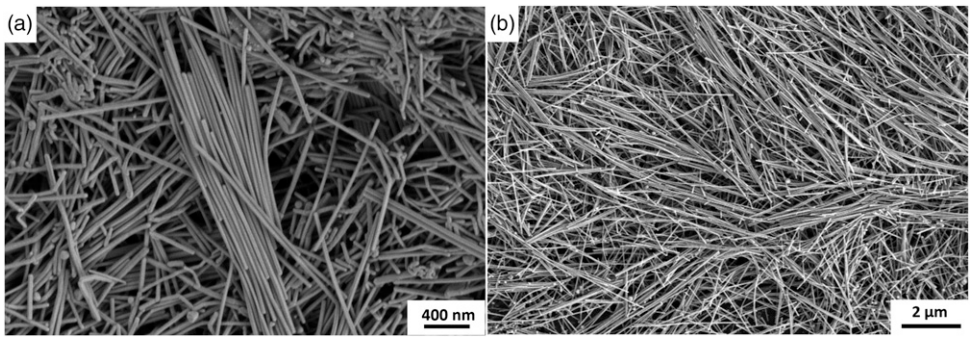

Figure 1. SEM images of synthesized AgNW networks on a glass substrate with (a) high and (b) low amplification.

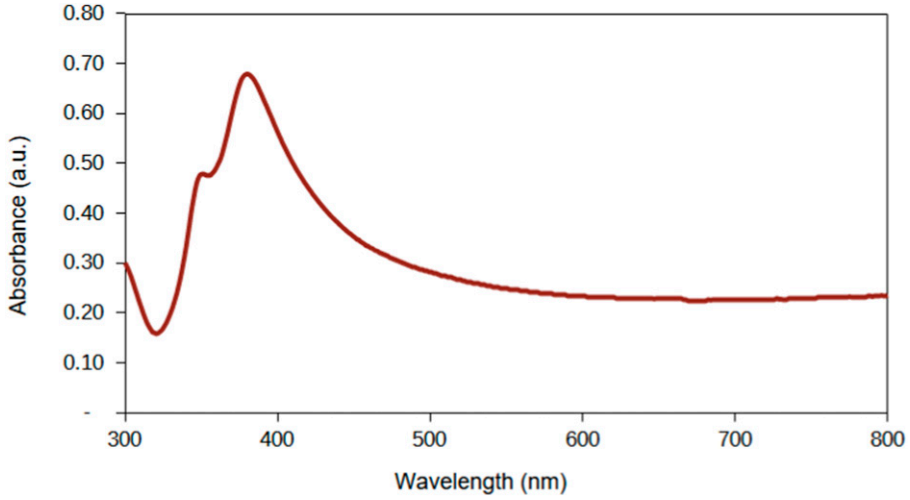

Figure 2. UV-visible absorption spectra of the synthesized AgNW colloidal solution.

Morphology of epoxy – AgNW composites

The morphology of fracture surfaces of the epoxy and the composites were investigated using SEM. Images of the surfaces are given in Figure 3. It was observed that while some riverlines have been seen on the surface of the neat epoxy (Figure 3(a)), fracture surfaces of nanocomposites are quite rough and have a greater number of riverlines (Figure 3(b)–(f)), which indicates a comparatively substantial amount of deformation of the polymer matrix. Higher deformation of the polymer may have resulted from the interaction of several micromechanisms for toughening and strengthening brought on by the presence of AgNW in epoxy.[35] Strong riverlines and deflection of the fracture plane in the 0.25 wt% modified AgNW composite (Figure 3(e)) demonstrate ductile failure evidence. When the AgNW loading increased to 0.25 wt%, the failure mode of the nanocomposite changed. A dense rough surface was observed in samples with 0.25 wt% modified AgNWs whereas much uniformer and rougher surfaces were observed in composites with unmodified AgNWs. EDS investigations were performed to comprehend the AgNW distribution in the epoxy matrix. Figure 4 displays EDS mapping images for the elements on the surface of the 5 wt % AgNW-epoxy composite. AgNW agglomerates are visible on the surface, as shown in Figure 4(b) which could result in poor physical properties for the composites. On the other hand, AgNWs are not visible for composites with AgNW levels less than 5 wt%. Thus, only at the highest concentration, agglomerations are visible.

FTIR study of epoxy – AgNW composites

FTIR analysis was used to examine organic structures of modified AgNW and composites prepared with AgNWs added to the epoxy resin at different reinforcement ratios presented in Figure 5. No significant absorption peaks were observed for unmodified AgNWs in the FTIR spectra. Modified AgNW provided more pronounced absorption

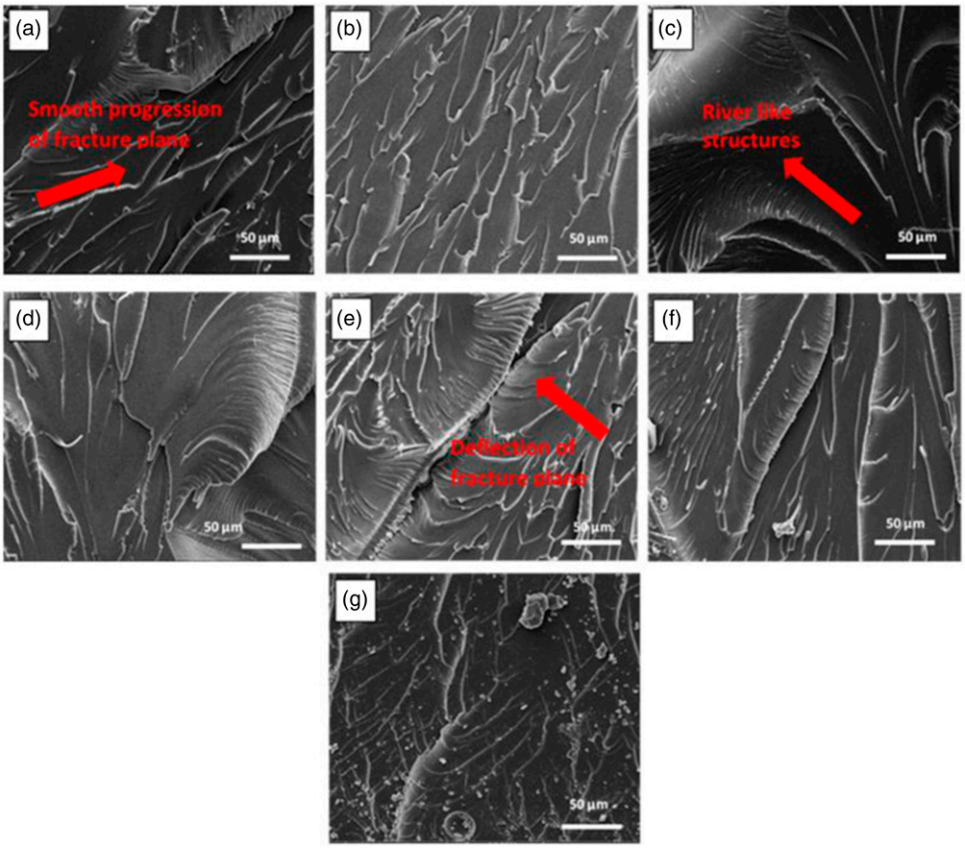

Figure 3. SEM images of fracture surfaces of (a) the epoxy, (b) 0.05, (c) 0.10, (d) 0.25 wt% AgNW composites, (e) 0.25 wt% modified AgNW, (f) 0.50 wt% AgNW and (g) 5 wt% AgNW composites.

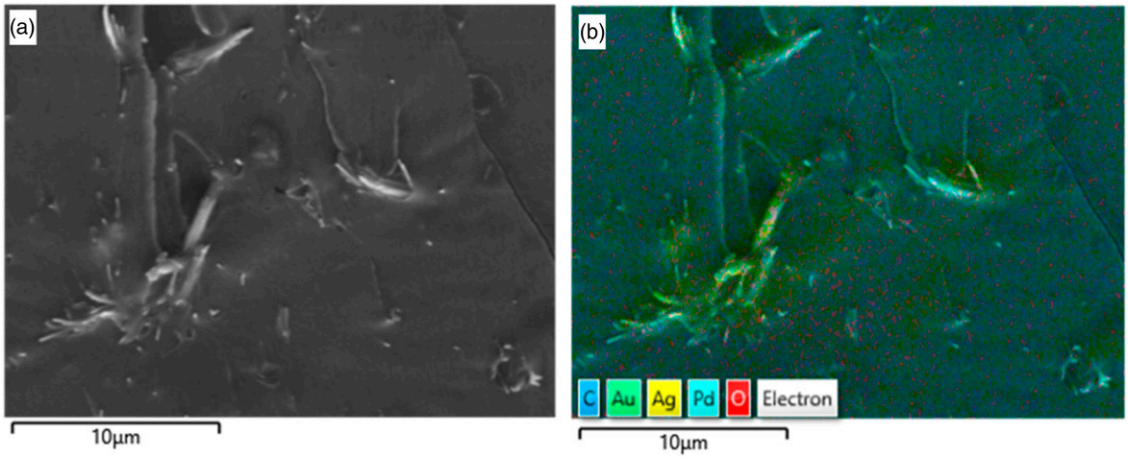

Figure 4. EDS analysis for the 5 wt% AgNW integrated composite, i.e., (a) electron image and (b) EDS layered image, where the yellow color indicates silver atoms.

peaks than AgNW at vibrations of 1666 $c\text{m}^{-1}$ (-COOH), 1386 $c\text{m}^{-1}$ (-OH), 1085 $c\text{m}^{-1}$ (-COO) and 1045 $c\text{m}^{-1}$ (alkyl). Peaks were observed at 1238 and 813 $c\text{m}^{-1}$ related to the epoxy component (-C-O-C-) of the polymer resin. It was observed that peak intensities decreased with the addition of AgNW to the resin while the peak of the O = C = O vibration of the hardener of the epoxy resin was detected at 2349 $c\text{m}^{-1}$. There is a decrease in the peak intensity with the increase of AgNW integration. This may be due to the elimination of organic structures by agglomerations formed

by increasing the amount of nanomaterials in the structure. Closer inspection reveals that the decrease in peak intensities is high especially at 1743, 1238, 1109 cm^{-1} (-RCOO) and 1031 cm^{-1} (-CN) vibrations. Considering all FTIR peaks results in the finding that no new peaks were formed by the epoxy matrix or nanomaterials. Thus, obtained structures are composites.

Mechanical properties of epoxy – AgNW composites

In order to understand effects of nanowire addition and surface modification of nanowires, flexural analyses were carried out. The average of the flexural bending test with incorporated standard deviations are presented in Figure 6. Although there are slight differences in average values of the flexural strength, the strongly overlapping standard deviations indicate that the flexural strength of the epoxy composites are not affected by AgNWs. On the other hand, surface modification of AgNWs affects the mechanical properties of the epoxy resin strongly. A 46 % improvement in the flexural strength is achieved with the incorporation of 0.25 wt% surface modified AgNWs. This can be explained by the formation of covalent bonds between carboxyl groups on the surface of modified AgNWs and phenol groups of the epoxy resin.[36] In addition, the enhanced wetting of the surface of the nanoparticles may lead to better dispersion of them inside the matrix, thus enhancing the flexural strength.[35] According to these results, a small amount of AgNW incorporation into the epoxy resin can improve the mechanical properties due to sufficient load transfer from matrix to matrix – nanomaterial interface. These better mechanical results also prove that the interaction between polymer matrix and nanomaterial is the dominant mechanism on mechanical properties of the

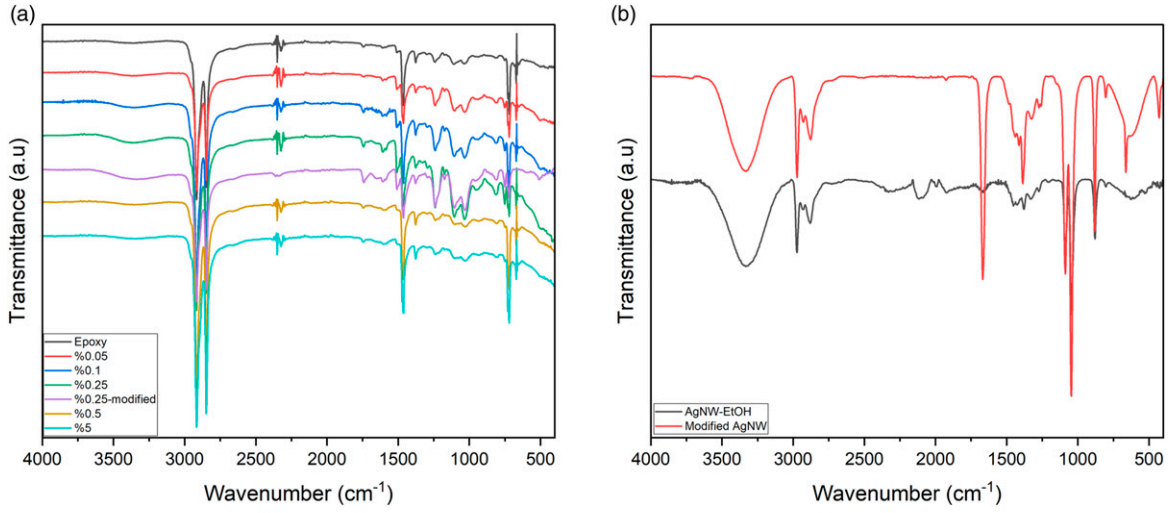

Figure 5. FTIR graphics of (a) nanocomposites and (b) modified AgNWs.

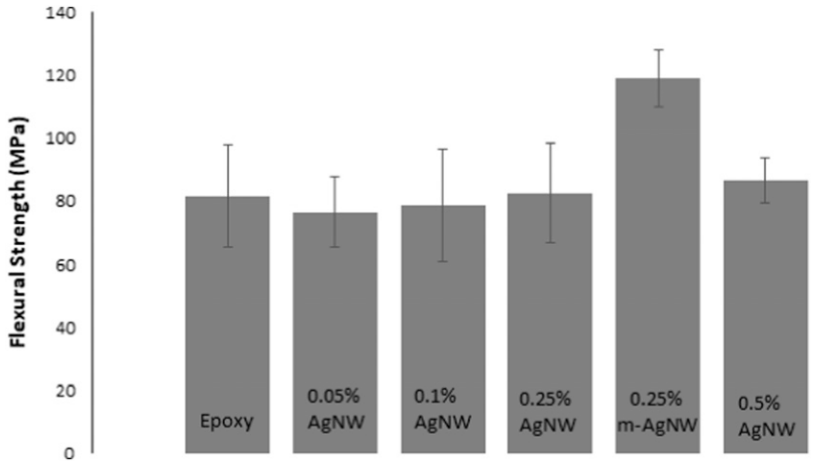

Figure 6. Flexural strengths of the epoxy and the epoxy-AgNW composites.

composites. SEM images of crack surfaces of the composites after the flexural loading presented previously in Figure 3(e) also prove that the the failure of the composite with modified AgNWs resulted in a rougher surface which indicates an improved stress transfer.

Thermal properties of epoxy – AgNW composites

Figure 7 represents thermal decomposition curves of the epoxy and the epoxy – AgNW composites. All of the samples seem to exhibit a one-step degradative behavior. However, derivative thermogravimetric (DTG) analysis reveals that the reaction took place in two steps, the first was the degradation of the secondary hydroxyl group on the propyl chain while the second was the degradation of the bisphenol-A group on the epoxy. Remarkably, these observations are in agreement with the literature.[37]

Results indicate further that the epoxy's thermal degredation behavior was not significantly changed by the addition of AgNWs. Note that the ineffectiveness of AgNW incorporation on the thermal stability of the polymer was also observed by Kim et al.[38] Temperatures at 5 % weight loss ($T_{d,\%5}$) and maximum weight loss ($T_{d,max}$) which were obtained from the first derivative of the weight loss versus temperature curves and the glass transition temperatures of the epoxy – AgNW composites are presented in Table 1.

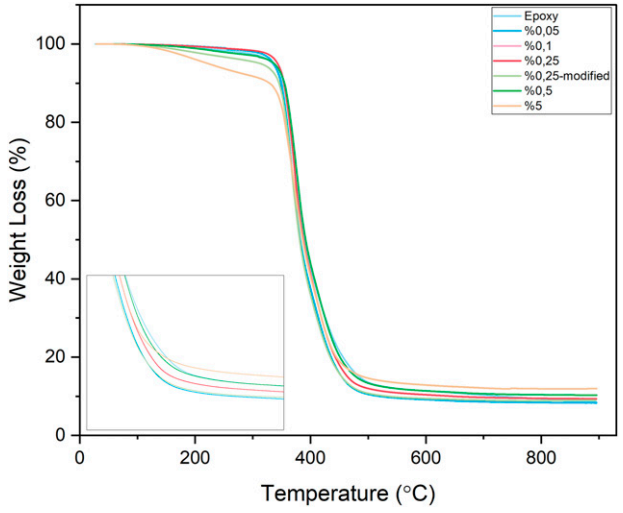

Figure 7. TGA curves of the neat epoxy and nanocomposites containing varying amounts of AgNWs, where the inset depicts the region between 400 and 600°C in detail.

According to these results, it was observed that temperatures at 5 % weight loss corresponding to the epoxy did not change with the incorporaton of AgNWs at low concentrations. On the other hand, a dramatic decrement was observed with the addition of 5 wt% AgNW. Feng et al.[39] also obtained similar results for epoxy – AgNW composites. This discovery can be explained by the precense of AgNWs with higher thermal conductivity compared to the epoxy matrix, which may act as heat dispersing sources during early stages of thermal deterioration. Contrarily, temperatures at maximum weight loss did not change significantly by AgNW addition. This can be explained with the absence of covalent interactions between nanowires and the matrix network. The mechanism of the dispersion is just the entanglement of nanowires with the polymer framework.

Furthermore, glass transition temperatures were determined via DSC analyses. According to Table 1, the glass transition temperature increases with the incorporation of AgNWs at low concentrations. This is due to the restricted mobility of polymer chains by the incorporation of more stiff nanowires. However, the composite with 5 wt% AgNW has a lower glass transition than the neat polymer which can be explained with the suppressed crosslinking reaction by the presence of nanowires. The epoxy matrix has a reduced crosslinking density and a higher chain mobility. As a result, nanocomposites glass transition temperature is lower than the neat polymer.[40] Furthermore, the composite with modified nanowires also shows a slightly lower glass transition temperature. This can be due to the free volume[41] that was added by the interaction of the carboxyl group of nanowires and phenol groups of the epoxy resin.

The thermal stability was also examined using the Integral Procedure Decomposition Temperature (IPDT) method[42,43] for verifying TGA results. According to this examination also presented in Table 1, it can be concluded that the thermal stability of the samples remained almost

Table 1. Thermal properties of epoxy and epoxy-AgNW composites.

Sample	$T_{d,\%5}$ [°C]	$T_{d,max}$ [°C]	T_g [°C]	IPDT [°C]
Epoxy	334	372	114	534
0.05 % AgNW – Epoxy	336	367	115	515
0.1 % AgNW – Epoxy	337	367	117	559
0.25 % AgNW – Epoxy	343	372	129	540
0.25 % modified AgNW – Epoxy	313	368	121	523
0.5 % AgNW – Epoxy	337	375	131	558
5 % AgNW – Epoxy	222	371	112	578

unaffected. A slight increase in the the thermal stability for increasing amounts of AgNWs is determined which is also observable in Figure 7 since the char yield increases with higher amounts of AgNWs due to the correspondingly higher thermal conductivity which in turn leads to higher heat release rates.

Electrical conductivity of epoxy – AgNW composites

As part of the electrical characterizations of hybrid films, we measured the electrical resistivity ρ of pure epoxy, epoxy composites with AgNW additives, and surface sanded AgNW (AgNW-ss) integrated composite samples (Figure 8)

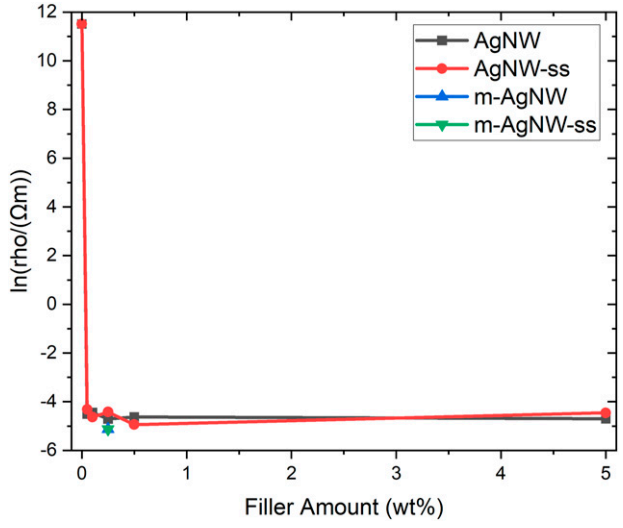

Figure 8. Logarithmic electrical resistivity values of AgNW and AgNW-ss integrated composites for varying filler amounts while for 0.25 wt% results for modified AgNW integrated samples with and without surface sanding denoted as m-AgNW and m-AgNW-ss are also depicted.

which exhibit a sharp decline for low amounts of fillers. These results clearly indicate that the percolation threshold value, which marks the insulator to conductor transition in three dimensional systems, was reached by adding 0.05 wt % AgNWs to the pure epoxy. Correspondingly, added nanowires improved the conductivity of the composites drastically by 10^6 folds at the lowest reinforcement ratio compared to the insulating state of the pure epoxy which highlights the electrical percolation effect driven by $\rho \propto (x - x_c)^t$, where x_c is the percolation threshold and t the critical exponent. Remarkably, the very low percolation threshold verifies the high aspect ratio of AgNWs.[44] Furthermore, conductivities above the percolation threshold lie around 10^2 S/m which is comparable to results obtained in the literature for various polymer matrices.[45,46] Hence, this value seems to be independent from the physical structure or the absolute permittivity of the polymer.

Note that results vary within the standard deviation of the experiment above the percolation threshold. Thus, no clear advantage or disadvantage is detectable for AgNW-ss introduced samples. However, 0.25 wt% modified AgNW integrated samples exhibit enhanced electrical conductivities in comparison to 0.25 wt% AgNW added samples, i.e., electrical conductivities are increased by 51 and 68% with and without surface sanding, respectively, which might be observable since better distribution of the nanomaterial was obtained for these samples.

EMI shielding performance of epoxy – AgNW composites

Figure 9 depicts the variation in transmission and reflection loss values of the epoxy and its nanocomposites with the *X*-band frequency range of 8.2 to 12.0 *G*Hz. It can be seen that the frequency only has a weak influence on the

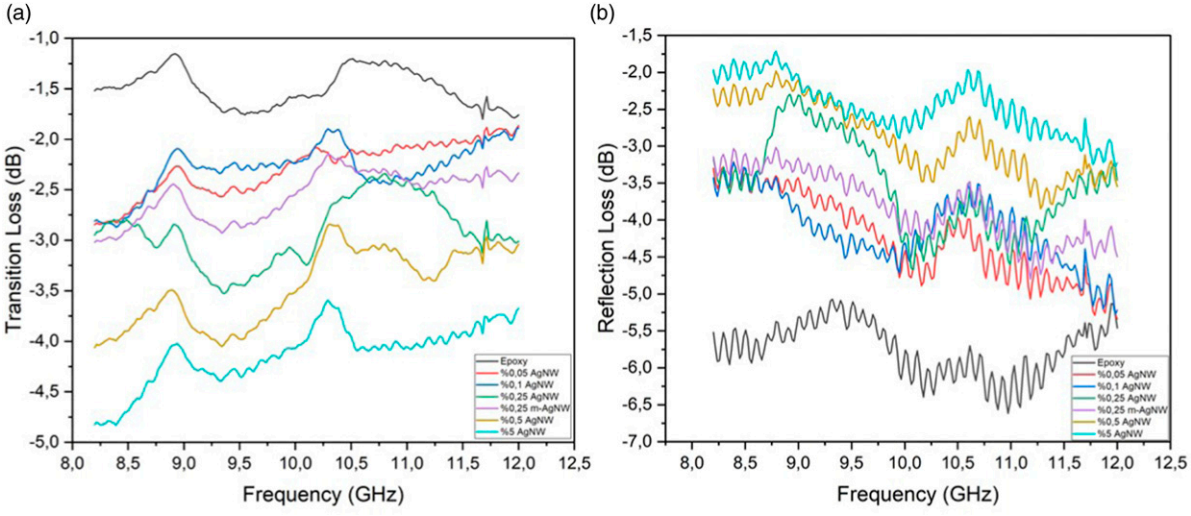

Figure 9. (a) Transmission loss and (b) reflection loss values of the epoxy and epoxy – AgNW composites.

Table 2. Electromagnetic properties of the epoxy and epoxy – AgNW composites.

Sample	Transmission *T* (%)	Reflection *R* (%)	Absorption *A* (%)	EMI SE (*d*B)
Epoxy	70.90	26.65	2.46	3.49
0.05 wt % AgNW – epoxy	59.13	37.63	3.24	7.17
0.1 wt % AgNW – epoxy	59.08	38.66	2.26	7.18
0.25 wt % AgNW – epoxy	51.10	44.35	4.55	9.30
0.25 wt % modified AgNW – epoxy	55.53	41.59	2.88	8.15
0.5 wt % AgNW – epoxy	45.05	51.45	3.50	10.79
5 wt % AgNW – epoxy	38.66	56.77	4.56	12.31

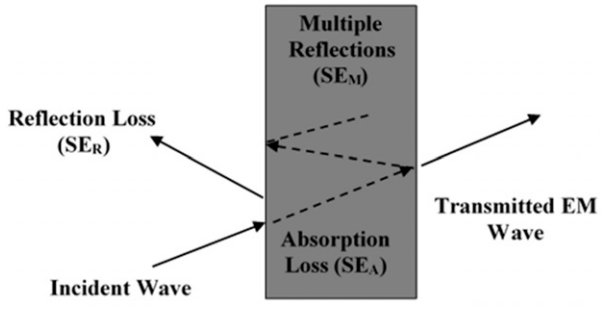

Figure 10. Shielding phenomena.

transmission and reflection loss values of the composites. In general, the transmission loss decreases while the AgNW loading degree increases in the composites. Conversely, reflection loss values increase with higher AgNW loadings. Percent transmission, reflection and absorption values of the epoxy and nanocomposites were computed using average transmission loss values in equation (1) which is presented in Table 2. According to these results, with just a 0.05 wt% AgNW loading, the average transmission of the epoxy composites decreases to 59.13 % from 70.90% which is in parallel with observations obtained from the electrical conductivity measurements. Additionally, when the AgNW loading degree is 5 wt%, a minimum transmission of 38.66 % is attained. Note that the increase in electrical conductivity, which is directly linked to the rise in the composites' AgNW loading degree is the cause of the transmission decrease due to the Schelkunoff theory,[26] which states that the total EMI shielding effectiveness SE can be decomposed in three parts, i.e., attenuation from reflection (SE_R), multiple reflections (SE_M) which is negligible in most cases and absorption (SE_A). Corresponding shielding phenomena are depicted in Figure 10.

Remarkably, SE_R and SE_A depend on the total conductivity σ by equation (3), i.e.,

$$SE_R \propto \ln \sigma, SE_A \propto \sqrt{\sigma}, SE_M \propto \ln\left(1 - 10^{\frac{SE_A}{10}}\right). \quad (3)$$

Hence, an increasing conductivity leads to an increasing EMI shielding effectiveness.

It can be observed that both percent reflection and absorption values of the epoxy are increasing with the addition of AgNWs. However, the main EMI shielding mechanism seems to be the reflection due to the reflective characteristics of silver. It can be observed from Table 2 that the EMI SE of the plain epoxy was increased 3.5 fold with the addition of 5 wt% AgNWs. Altough the EMI SE of the composite in the *X*-band is relatively low for several applications, it should be remembered that, in this study, the epoxy resin is not combined with carbon fibers. Correspondingly, the EMI SE of CFRPs with AgNWs would be far higher than 12.31 dB.

Conclusions

In this study, we aimed to develop a composite for usage in carbon fiber reinforced polymers that contains up to 5 wt% AgNWs and an aerospace grade epoxy resin. The study's major goal was to increase the composite's electrical conductivity while keeping its mechanical and thermal qualities in order to improve the shielding performance against EMI. Physical properties of solid composites were enhanced by altering surfaces of AgNWs to boost their capacity to disperse in epoxy. As a result of the study, it was found that the inclusion of AgNWs had little effect on the flexural strength of the epoxy, while the composite with surface-modified AgNWs outperformed the epoxy by 46% due to the enhanced interaction between matrix and nanoparticles. The electrical conductivity of the resin was dramatically improved by the addition of AgNWs at the lowest reinforcement ratio by 10^6 folds. The transmission value of the epoxy resin in the *X*-band decreased from 70.90 to 38.66% with the incorporation of 5 wt % AgNWs. The decreasing trend of transmission values by increasing the AgNW content adresses the aim of tunable shielding performance for the composite with variable nanoparticle loading. It can be concluded that AgNWs enhanced the aerospace grade epoxy resin's mechanical, electrical, and electromagnetic properties, proving the usefulness of AgNWs as a CFRP reinforcing material.

Acknowledgements

Authors would like to thank Turkish Aerospace, Nanografi Nano Technology, the Institute of Materials Science and

Nanotechnology at Bilkent University and NANOME for providing the necessary infrastructure and support. Finally, we thank to A. T. Astarlıoğlu for his support on the network analyzer measurements.

Declaration of conflicting interests

The author(s) declared no potential conflicts of interest with respect to the research, authorship, and/or publication of this article.

Funding

The author(s) disclosed receipt of the following financial support for the research, authorship, and/or publication of this article: Authors gratefully acknowledge financial support by the Scientific and Technological Research Council of Turkey within the 1004 program (project ns. 20AG001, 20AG020 and 20AG026).

ORCID iDs

Merve Özkutlu Demirel https://orcid.org/0000-0002-3176-4842
Talha Erdem https://orcid.org/0000-0003-3905-376X
Yahya Öz https://orcid.org/0000-0003-3784-0495

Data availability statement

Data sharing not applicable to this article as no datasets were generated or analyzed during the current study.

References

1. Iqbal K, Khan S-U, Munir A, et al. Impact damage resistance of CFRP with nanoclay-filled epoxy matrix. *Compos Sci Technol* 2009; 69(11–12): 1949—1957.
2. Maccaferri E, Ortolani J, Mazzocchetti L, et al. New application field of polyethylene oxide: PEO nanofibers as epoxy toughener for effective CFRP delamination resistance improvement. *ACS Omega* 2022; 7(27): 23189–23200.
3. Zhang X, Sun T, Lei Y, et al. Synergistically optimizing interlaminar behavior of CFRP composites by simultaneously applying amino-rich graphene oxide to carbon fiber and epoxy matrix. *Compos Appl Sci Manuf* 2021; 145: 106372.
4. Karaboğa F, Göleç F, Yunus DE, et al. Mechanical response of carbon fiber reinforced epoxy composite parts joined with varying bonding techniques for aerospace applications. *Compos Struct* 2024; 331: 117920.
5. Nam S, Cho HW, Lim S, et al. Enhancement of electrical and thermomechanical properties of silver nanowire composites by the introduction of nonconductive nanoparticles: experiment and simulation. *ACS Nano* 2013; 7(1): 851–856.
6. Öztürkmen MB, Özkutlu Demirel M, Ağaç Ö, et al. Tailored multifunctional nanocomposites obtained by integration of carbonaceous fillers in an aerospace grade epoxy resin curing at high temperatures. *Diam Relat Mater* 2023; 135: 109840.
7. Öztürkmen MB, Öz Y and Dilsiz N. Physical and mechanical properties of graphene and h-boron nitride reinforced hybrid aerospace grade epoxy nanocomposites. *J Appl Polym Sci* 2023; 140(45): e54639.
8. Zeng Z, Chen M, Pei Y, et al. Ultralight and flexible polyurethane/silver nanowire nanocomposites with unidirectional pores for highly effective electromagnetic shielding. *ACS Appl Mater Interfaces* 2017; 9(37): 32211–32219.
9. Thomassin J-M, Jérôme C, Pardoen T, et al. Polymer/carbon based composites as electromagnetic interference (EMI) shielding materials. *Mater Sci Eng R Rep* 2013; 74(7): 211–232.
10. Schuster A, Larsen L, Fischer F, et al. Smart manufacturing of thermoplastic CFRP skins. *Procedia Manuf* 2018; 17: 935–943.
11. Zhang X, Hao H, Shi Y, et al. Static and dynamic material properties of CFRP/epoxy laminates. *Construct Build Mater* 2016; 114: 638–649.
12. Ma Z, Kang S, Ma J, et al. Ultraflexible and mechanically strong double-layered aramid nanofiber–$Ti_3C_2T_x$ MXene/silver nanowire nanocomposite papers for high-performance electromagnetic interference shielding. *ACS Nano* 2020; 14(7): 8368–8382.
13. Bedel V, Lonjon A, Dantras E, et al. Influence of silver nanowires on thermal and electrical behaviors of a poly (epoxy) coating for aeronautical application. *J Appl Polym Sci* 2018; 135(47): 46829.
14. Gao X, Lee HM, Ewe W-B, et al. Electromagnetic characterization and measurement of conductive aircraft CFRP composite for lightning protection and EMI shielding, TechRxiv. 2022. doi:10.36227/techrxiv.21701348.v
15. Wang L, Ma Z, Zhang Y, et al. Polymer-based EMI shielding composites with 3D conductive networks: a mini-review. *SusMat* 2021; 1(3): 413–431.
16. Öz Y. A mathematical model for the description of the electrical conductivity of graphene/polymer nanocomposites. *J Phys : Conf Ser* 2021; 1730: 012112.
17. Fang F, Li Y-Q, Xiao H-M, et al. Layer-structured silver nanowire/polyaniline composite film as a high performance X-band EMI shielding material. *J Mater Chem C Mater* 2016; 4(19): 4193–4203.
18. Jiang H, Moon K-s., Li Y, et al. Surface functionalized silver nanoparticles for ultrahigh conductive polymer composites. *Chem Mater* 2006; 18(13): 2969–2973.
19. Öz Y, Yilmaz B and Evis Z. A review on nanocomposites with graphene based fillers in poly(ether ether ketone). *Polym Sci, Series A*. 2022; 64(3): 145–160.
20. Asiaei S, Khatibi AA, Baniasadi M, et al. Effects of carbon nanotubes geometrical distribution on electrical percolation of nanocomposites: a comprehensive approach. *J Reinforc Plast Compos* 2010; 29(6): 818–829.
21. Alizadeh Sahraei A, Ayati M, Baniassadi M, et al. Ac and dc electrical behavior of mwcnt/epoxy nanocomposite near percolation threshold: equivalent circuits and percolation limits. *J Appl Phys* 2018; 123(10): 105109.
22. Chen C, Tang Y, Ye YS, et al. High-performance epoxy/silica coated silver nanowire composites as underfill material for electronic packaging. *Compos Sci Technol* 2014; 105: 80–85.

23. Zheng X, Zhang H, Liu Z, et al. Functional composite electromagnetic shielding materials for aerospace, electronics and wearable fields. *Mater Today Commun* 2022; 33: 104498.
24. Yu Y-H, Ma C-CM, Teng C-C, et al. Electrical, morphological, and electromagnetic interference shielding properties of silver nanowires and nanoparticles conductive composites. *Mater Chem Phys* 2012; 136(2–3): 334–340.
25. Chaudhary V. High performance X-band electromagnetic shields based on methyl-orange assisted polyaniline-silver core-shell nanocomposites. *Polymer-Plastics Technology and Materials* 2021; 60(14): 1–10.
26. Wanasinghe D and Aslani F. A review on recent advancement of electromagnetic interference shielding novel metallic materials and processes. *Compos B Eng* 2019; 176: 107207.
27. Öztürkmen MB, Özkutlu Demirel M and Öz Y. Investigation of mechanical and physical properties of graphene with epoxy matrix. *Eskişehir Technical University Journal of Science and Technology A - Applied Sciences and Engineering* 2021; 22: 112–119.
28. Kim T, Canlier A, Kim GH, et al. Electrostatic spray deposition of highly transparent silver nanowire electrode on flexible substrate. *ACS Appl Mater Interfaces* 2013; 5(3): 788–794.
29. Wang C, Murugadoss V, Kong J, et al. Overview of carbon nanostructures and nanocomposites for electromagnetic wave shielding. *Carbon* 2018; 140: 696–733.
30. Erdogan N, Erden F, Astarlioglu AT, et al. Ito/au/ito multilayer thin films on transparent polycarbonate with enhanced emi shielding properties. *Curr Appl Phys* 2020; 20(4): 489–497.
31. Kumar A, Shaikh MO and Chuang C-H. Silver nanowire synthesis and strategies for fabricating transparent conducting electrodes. *Nanomaterials* 2021; 11(3): 693.
32. Fahad S, Yu H, Wang L, et al. Recent progress in the synthesis of silver nanowires and their role as conducting materials. *J Mater Sci* 2019; 54(2): 997–1035.
33. Sun Y. Silvernanowires - unique templates for functional nanostructures. *Nanoscale* 2010; 2(9): 1626–1642.
34. Ramasamy P, Seo D-M, Kim S-H, et al. Effects of TiO_2 shells on optical and thermal properties of silver nanowires. *J Mater Chem* 2012; 22(23): 11651–11657.
35. Rathore DK, Prusty RK and Ray BC. Mechanical, thermomechanical, and creep performance of cnt embedded epoxy at elevated temperatures: an emphasis on the role of carboxyl functionalization. *J Appl Polym Sci* 2017; 134(21): 44851.
36. De S, Fulmali AO, Shivangi P, et al. Interface modification of carbon fiber reinforced epoxy composite by hydroxyl/carboxyl functionalized carbon nanotube. *Mater Today Proc* 2020; 27(2): 1473–1478.
37. Sovizi MR, Fakhrpour G and Madram AR. Comparison of thermal degradation behavior of epoxy/ammonium perchlorate composite propellants. *J Therm Anal Calorim* 2017; 129(1): 401–410.
38. Kim TG, Kim JM, Jang K-S, et al. Dispersibility-tailored conductive epoxy nanocomposites with silica nanoparticle-embedded silver nanowires. *Polym Test* 2021; 96: 107111.
39. Feng Y, Li X, Zhao X, et al. Synergetic improvement in thermal conductivity and flame retardancy of epoxy/silver nanowires composites by incorporating "branch-like" flame-retardant functionalized graphene. *ACS Appl Mater Interfaces* 2018; 10(25): 21628–21641.
40. Wang S, Tambraparni M, Qiu J, et al. Thermal expansion of graphene composites. *Macromolecules* 2009; 42(14): 5251–5255.
41. Yadav A, Kumar A, Singh PK, et al. Glass transition temperature of functionalized graphene epoxy composites using molecular dynamics simulation. *Integrated Ferroelectrics Int J* 2018; 186(1): 106–114.
42. Doyle CD. Estimating thermal stability of experimental polymers by empirical thermogravimetric analysis. *Anal Chem* 1961; 33(1): 77–79.
43. Zotti A, Zuppolini S, Borriello A, et al. Thermal and mechanical characterization of an aeronautical graded epoxy resin loaded with hybrid nanoparticles. *Nanomaterials* 2020; 10(7): 1388.
44. Nguyen THL, Quiroga Cortes L, Lonjon A, et al. High conductive Ag nanowire–polyimide composites: charge transport mechanism in thermoplastic thermostable materials. *J Non-Cryst Solids* 2014; 385: 34–39.
45. Alvarez MP, Poblete VH, Pilleux ME, et al. Submicron copper-low-density polyethylene conducting composites: structural, electrical, and percolation threshold. *J Appl Polym Sci* 2006; 99(6): 3005–3008.
46. Lonjon A, Demont P, Dantras E, et al. Low filled conductive P(VDF-TrFE) composites: influence of silver particles aspect ratio on percolation threshold from spheres to nanowires. *J Non-Cryst Solids* 2012; 358(23): 3074–3078.